RSC Advances

This is an *Accepted Manuscript*, which has been through the Royal Society of Chemistry peer review process and has been accepted for publication.

Accepted Manuscripts are published online shortly after acceptance, before technical editing, formatting and proof reading. Using this free service, authors can make their results available to the community, in citable form, before we publish the edited article. This *Accepted Manuscript* will be replaced by the edited, formatted and paginated article as soon as this is available.

You can find more information about *Accepted Manuscripts* in the Information for Authors.

Please note that technical editing may introduce minor changes to the text and/or graphics, which may alter content. The journal's standard Terms & Conditions and the Ethical guidelines still apply. In no event shall the Royal Society of Chemistry be held responsible for any errors or omissions in this *Accepted Manuscript* or any consequences arising from the use of any information it contains.

ROYAL SOCIETY OF CHEMISTRY

www.rsc.org/advances

RSC Advances RSCPublishing

ARTICLE

Transition of the electrostatic potential from the inside of an open channel to the reservoir

Cite this: DOI: 10.1039/x0xx00000x

Chun-Fei Kung[a,c], Chang-Yi Wang[b] and Chien-Cheng Chang[a,c,*]

Received 00th January xxxx,
Accepted 00th January xxxx

DOI: 10.1039/x0xx00000x

www.rsc.org/

Analytic work for electric double layer (EDL) is often pursued for an infinite channel. But in reality the channel must be finite in length. The note is aimed to address how the electrostatic EDL potential near the open edge of a channel is affected by the boundary conditions on the end walls and the location where we specify the reservoir condition. The analysis is performed under the Debye-Hückel approximation, which enables us to solve for the EDL potential by a semi-analytical approach. Two non-dimensional transition lengths are defined to characterize the effects near the open edge: the inner transition distances d_i and the outer transition distance d_o, in particular, we report their dependence on the non-dimensional electro-kinetic width K under various conditions. It is found that the inner d_i is of the order unity for small K, reaches its maximum for K near 1 or less, and decreases monotonically with increasing K. On the other hand, the outer d_o for small K could be the same order as the normalized distance from the open edge to the reservoir, and decreases monotonically with increasing K. These different transition behaviours on the two different sides of the channel edge are explained with the collaboration effects among the imposed boundary conditions.

Introduction

In the past years, we have seen that microfluidic devices are finding growing applications in modern technologies, such as microbiological sensors and micro-electro-mechanical systems[1]. One of the principles is to use the EDLs in a micron- or nano-scale channel to transport, mix or separate electrolytes by externally applying a steady or time-varying voltage. There have been extensive publications regarding theoretical analysis of novel devices; yet most of the analytical studies for electric double layers (EDLs) are pursued for infinite-length channels. Analytical solutions for EDLs under the Debye–Hückel approximation include circular cross section[2], parallel plates[3], and the rectangular cross section (in infinite series[4-6]). Keh et al.[7] present the analytical solutions in closed forms obtained with the cylindrical cell model. For all other cross sections, semi-analytical methods with boundary collocations[9] or even fully numerical methods such as finite elements[8] must be used.

The interest of the present study is to pursue a semi-analytical study for investigating the electrostatic EDL potential at the edge of an open channel. The edge is where the channel is open to the external environment (reservoir), which necessarily modifies the EDL potential inside the channel. In addition, there are also boundary conditions on the end walls of the channel (cf. Fig 1), which the electrostatic potential must satisfy. Naturally, we inquire about (1) how deep into the channel (from the edge) is the EDL potential affected? and (2) how quickly (from the edge) does the electrostatic EDL potential modify itself to satisfy the reservoir condition? In other words, we investigate the transition of the EDL potential from deep inside the channel to the reservoir. We shall define two distances (normalized by one-half width of the channel) to characterize the transition: the inner transition distance (d_i) and the outer transition distance (d_o) (cf. Fig. 2).

It is worthwhile to review some recent devices using EDL potentials for applications among many others. Lee et al.[10] present a new electro-kinetically driven active micro-mixer which uses localized capacitance effects to induce zeta potential variations along the silica-based micro-channels. Their numerical and experimental results demonstrate that the developed microfluidic device permits a high degree of control over the fluid flow and an efficient mixing effect. Mahabadi et al.[11] present the fabrication of micro fluidic channels in PMMA by direct proton beam writing (PBW) and the experimental characterization of their electro-kinetic characteristics using the methods of current monitoring and particle image velocimetry (PIV). Kuo et al.[12] focus on the development of a bubble-free ac electro-kinetic microfluidic driver via the asymmetrically capacitance-modulated (ACM) microelectrode arrays, which can enhance the desired tangential electric field to control the local fluid and drive the micro-objects. Plecis et al.[13] propose a new approach for FlowField Effect Transistors (FFETs) by using polarizable interfaces indirect contact with the electrolyte. This is a method for precise control of electro-osmotic flow. And the concept will be interesting for the development of highly programmable microfluidic separation devices. Fine et

RSC Advances Accepted Manuscript

al.[14] elucidates the potential of important new therapeutic paradigms, including metronomic delivery and chronotherapy. They present an actively controlled nano-fluidic membrane that exploits electrophoresis to control the magnitude, duration, and timing of drug release. These examples are all related to the use of electro-osmosis or electrophoresis which heavily replies on the EDL potentials. All the applications in practical micro-fluidic devices necessarily use channels of finite lengths for which the effects of open edges need to be addressed. The effects are also important in the assessment of the access resistance of small pores[15-16].

The model problems

To address the effects of an open channel (necessarily with end walls), as shown in Fig. 1a-b, we consider three boundary conditions to be specified in (15). Fig. 1a shows two-dimensional periodic channels between two large reservoirs. Normalize all lengths by the half channel width L. After normalization by the zeta potential ζ of the side walls, the EDL potential on the channel walls becomes 1, and the reference potential is set to be 0 on the reservoir walls. The period of the channels is $2bL$ (b>1) and the reservoir wall is cL from the channel. Fig. 1b shows the end region where the origin of the Cartesian coordinates is placed at the centre of the exit. We separate a period of the domain to two regions. Region 1 ($-\infty < x < 0,\ |y| \le 1$) is inside the channel; Region 2 ($0 < x < c,\ |y| \le b$) is between the exit and the reservoir.

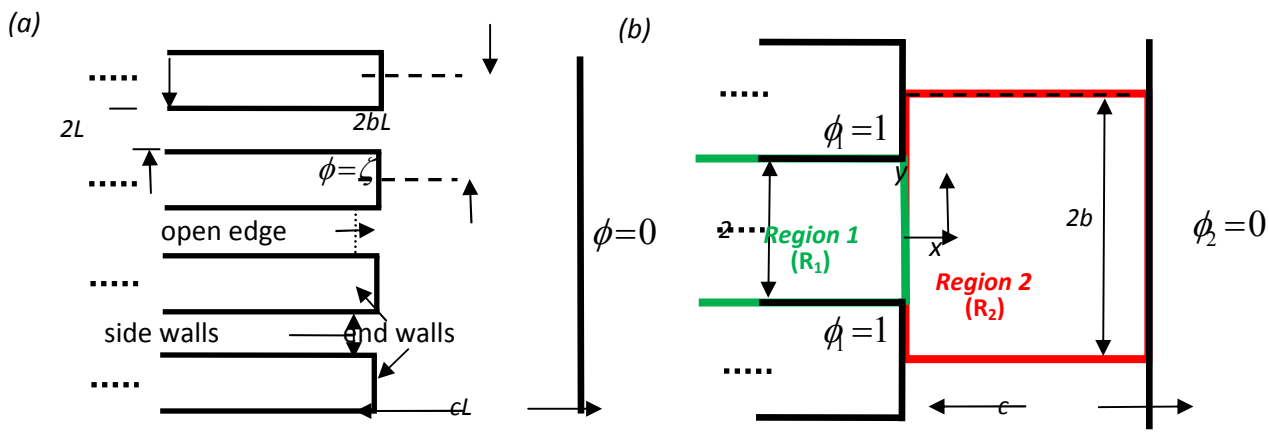

Fig 1. Schematic of the physical problem with the coordinates specified on the right panel: (a) An array of open channels considered is made periodic in the y-direction with $2L$ the channel width and $2bL$ the length of a period. The "reservoir" is at the distance cL from the open edges (or end walls). Note that the channels extend to infinity in the negative x-direction; (b) One period of a channel depicted in terms of the coordinates (x, y) (using L as the reference length) with the origin at the centre of the channel edge. Note that the region is divided to two sub-regions: R_1 and R_2. The side walls of the channel are given the same zeta potential value ζ, which is used to normalize the electrostatic EDL potential with ϕ ($x \le 0$; $y=\pm 1$)=1. As a remark for clarity, we simply say an infinite channel if the channel has no open edge, namely, its side walls extend to infinity in both positive and negative x-directions (and thus $c \to \infty$). Three cases of boundary conditions for the end walls are specified in (15).

Basic equations

Consider the problem of finding the EDL potential for a micro-channel. Let us start with Poisson's equation for the electrostatic system,

$$\nabla' \cdot \left(\varepsilon \nabla' \psi'\right) = -\rho_e \tag{1}$$

where ψ' is the electric potential, ε is the electric permittivity of the solution, and ρ_e is the charge density. The charge density can be expressed by

$$\rho_e = e\left(z_+ n_+ + z_- n_-\right) \tag{2}$$

where e (positive) denotes the proton charge, z_+ and z_- are the valences of cations and anions, and n_+ and n_- are the number concentrations of cations and anions, respectively. It is assumed that the concentrations of ions follow the Boltzmann distribution,

$$n_\pm = n_\pm(\mathbf{p}) \exp\left\{-\frac{e z_\pm}{k_b T}\left[\left(\psi' - \psi'(\mathbf{p})\right)\right]\right\} \tag{3}$$

This journal is © The Royal Society of Chemistry 2012
RSC Advances Accepted Manuscript

where **p** is a reference point, k_b is the Boltzmann constant, and T is the temperature.

For simplicity, a symmetric electrolyte is assumed, and **p** is chosen to the reference where the fluid is electro neutral. It is convenient to set $z_+ = -z_- = z_0$, $\psi'(\mathbf{p}) = 0$, and $n_+(\mathbf{p}) = n_-(\mathbf{p}) = n_0$, where n_0 is the number concentration of the bulk electrolyte. The point **p** for the zero reference potential $\psi'(\mathbf{p}) = 0$ need not be inside a channel, but must lie somewhere outside. It follows from Eqs. (1)-(3) that the electric potential ψ' obeys the Poisson–Boltzmann equation

$$\nabla' \cdot \left(\varepsilon \nabla' \psi'\right) = 2 z_0 e n_0 \sinh\left(\frac{z_0 e \psi'}{k_b T}\right) \tag{4}$$

In addition, we have $\psi' = \zeta$ at the wall (shear plane), where ζ is the zeta potential, a measurable electrical information. In the case of low values of zeta potential, i.e., small $z_0 e\zeta / k_b T$, we may linearize Eq. (4) and recast it into the non-dimensional form,

$$\nabla^2 \phi = K^2 \phi. \tag{5}$$

This is usually called the Debye–Hückel approximation. All the lengths are normalized by the characteristic channel dimension L, and we have normalized the electrostatic EDL potential by setting $\phi = \psi' / \zeta$. The parameter $K = L / \lambda_D$ with $\lambda_D = (k_b T / 2 z_0^2 e^2 n_0)^{1/2}$ the Debye length is sometimes called the non-dimensional electro-kinetic width[17–18]. Equations (1)-(5) can be found in a standard textbook in microfluidics; see, for example, in Chapter 7 of Ref. [19].

Apparently, K measures the relative thickness of the channel width (L) compared to the Debye length λ_D of the electric double layer. Hence we have relatively a wide channel if K is large and a thin one if K is small. In particular, the EDLs next to the two side walls overlap with each other, say, for K< 2, and are well separated, say, for K> 4. It is quite typical that K lies in the range 1-10^4 in capillary electrophoresis applications. Consider, for example, a microfluidic channel with width L=10nm~10μm where the Debye is in the range λ_D=1~10nm. Smaller K can be produced by using smaller micro-channels or decreasing the concentration of the bulk electrolyte. In particular, we present results for 0.2<K<20 which covers a range from overlapped EDLs (K< 2) to well-separated EDLs (K> 4).

The normalized Debye-Hückel equation in component form is

$$\phi_{xx} + \phi_{yy} - K^2 \phi = 0 \tag{6}$$

First of all, we consider the simple case of the channel between two infinite plates with $\phi(x, \pm 1) = 1$. It is known that the solution to Eq. (6) is given by

$$\phi = \frac{\cosh(Ky)}{\cosh(K)}, \tag{7}$$

and along the centreline (y=0), we have

$$\phi_0 = \frac{1}{\cosh(K)} \tag{8}$$

Next refer to the problem concerned in this study, as sketched in Fig. 1a-b. We shall find the (partial) solutions, respectively, for Regions 1 and 2 (necessarily with undetermined coefficients), and then match them at the channel edge to completely determine the solution.

For region 1 (R_1), the complete general solution to Eq. (6) that satisfies $\phi(x, \pm 1) = 1$ is given by

$$\phi_1 = \frac{\cosh(Ky)}{\cosh(K)} + \sum_1^\infty A_n \cos(\alpha_n y) e^{\tilde{\alpha}_n x} \tag{9}$$

where

$$\alpha_n = \left(n - \frac{1}{2}\right)\pi, \quad \tilde{\alpha} = \sqrt{\alpha_n^{\,2} + K^2} \tag{10}$$

The first term of (9) which satisfies the boundary condition is also solution to Eq. (6) for the infinite channel. The second term of (9), the complete Fourier series solution to Eq. (6) which must be identically zero on the side walls, is included to account for the open edge effect. Note that each term in (9) is an even function of y for we have considered symmetric boundary conditions on the two side walls.

For region 2 (R_2), the complete general solution to Eq. (6) that satisfies the reservoir condition $\phi = 0$ at x=c and the reflective conditions $\partial\phi / \partial y(x, \pm b) = 0$ is

$$\phi_2 = B_0 \sinh[K(x-c)] + \sum_1^\infty B_n \cos(\beta_n y) \sinh[\tilde{\beta}(x-c)] \tag{11}$$

where

$$\beta_n = \frac{n\pi}{b}, \quad \tilde{\beta}_n = \sqrt{\beta_n^{\,2} + K^2} \tag{12}$$

The first term of (11) is the solution to Eq. (6) that satisfies the zero reservoir condition, thus leaving an undetermined coefficient B_0. The second term of (11) is the complete Fourier series solution that satisfies the reflective conditions to account for periodic structure of the array of micro-channels in the y-direction.

The unknown coefficients A_n of (9) and B_n of (11) are determined by the conditions at the junction x=0 of regions 1 and 2, where we require continuity

RSC Advances Accepted Manuscript

$$\phi_1(0,y)=\phi_2(0,y) \qquad -1\le y\le 1 \tag{13}$$

$$\frac{\partial\phi_1}{\partial x}(0,y)=\frac{\partial\phi_2}{\partial x}(0,y) \qquad -1\le y\le 1 \tag{14}$$

On the end walls ($x=0,\ 1<|y|\le b$), we consider three cases:

$$\begin{cases}\text{Case 1: } \phi_2=0 \text{ (the same potential as in the reservoir);}\\ \text{Case 2: } \phi_2=1 \text{ (the same potential as on the side walls);}\\ \text{Case 3: } \dfrac{\partial\phi_2}{\partial x}=0 \text{ (namely, the end walls are insulated).}\end{cases} \tag{15}$$

Method of Collocation

We truncate the series A_n to N terms and B_n to M terms. For even spacing of the collocation points, let M=Integer(bN),

$$\begin{cases} y_j=\dfrac{(j-0.5)}{N}, & j=1\ to\ N,\ 0\le y_j<1\\ y_i=\dfrac{(i-0.5)}{M-N}(b-1)+1, & i=1\ to\ M-N,\ 1<y_i\le b\end{cases} \tag{16}$$

For Case 1, Eqs. (9), (11) subject to the conditions (13), (14) and (15) gives

$$\sum_{n=1}^{N}A_n\cos(\alpha y_j)+B_0\sinh(Kc)+\sum_{n=1}^{M-1}B_n\cos(\beta y_j)\sinh(\tilde{\beta}c)=-\frac{\cosh(Ky_j)}{\cosh(K)}, \quad j=1 \text{ to } N \tag{17}$$

$$\sum_{n=1}^{N}A_n\tilde{\alpha}\cos(\alpha y_j)-B_0K\cosh(Kc)-\sum_{n=1}^{M-1}B_n\tilde{\beta}\cos(\beta y_j)\cosh(\tilde{\beta}c)=0, \quad j=1 \text{ to } N \tag{18}$$

$$B_0\sinh(Kc)+\sum_{n=1}^{M-1}B_n\cos(\beta y_i)\sinh(\tilde{\beta}c)=0, \quad i=1 \text{ to } M\text{-}N \tag{19}$$

There are $M+N$ unknowns and $M+N$ linear equations, which are inverted easily.

For Case 2, Eq. (19) is replaced by

$$-B_0\sinh(Kc)-\sum_{n=1}^{M-1}B_n\cos(\beta y_i)\sinh(\tilde{\beta}c)=1,\ i=1\ to\ M-N \tag{20}$$

For Case 3, Eq. (19) is replaced by

$$B_0K\cosh(Kc)+\sum_{n=1}^{M-1}B_n\tilde{\beta}\cos(\beta y_i)\cosh(\tilde{\beta}c)=0,\ i=1\ to\ M-N \tag{21}$$

A typical convergence is shown in Table 1 where we examine the successive difference of the solutions with N=N_1 and N_2 over the entire computational domain R=$R_1\cup R_2$

$$e_\phi(N_1,N_2)=\left\{\frac{1}{\mathrm{R}}\int_{\mathrm{R}}\left[\phi(x,y|N_2)-\phi(x,y|N_1)\right]^2dxdy\right\}^{\frac{1}{2}}$$

where we recall M=Integer(bN) as the collocation is equal-spacing. In all the computations, it is sufficient to take N=250.

Table 1. Typical convergence of the three different cases: the successive difference $e_\phi(N_1,N_2)$ are listed for b=2 (M=2N), c=1, K=1.

(N_1 , N_2)	(50,100)	(100,150)	(150,200)	(200,250)
Case 1	8.612e-06	2.107e-06	7.756e-08	3.228e-08
Case 2	2.145e-06	1.142e-06	3.358e-07	6.914e-08
Case 3	4.310e-05	2.154e-05	1.154e-05	5.958e-06

Results and discussion

For illustration, the two transition distances d_i (inner) and d_o (outer) are graphically displayed in Fig. 2a. Here we compare the potential ϕ_c of the channel with an open edge to the potential ϕ_0 for the infinite channel (Eq. (8)) along the centreline (y=0). The inner transition distance d_i is measured from the channel edge toward the inside of the channel beyond which ϕ_c is 95% close or more to ϕ_0. The outer transition distance d_o is measured from the open edge toward the reservoir beyond which ϕ_c is smaller than 5% of ϕ_0. Note that d_i is limited to 1.5 which is less than one channel width (=2 in the non-dimensional unit) for all the three cases with b=2, c=5, K=1, while d_o is about 3.5 compared to c=5 where the reservoir condition is imposed. On the other hand, Fig. 2b shows the effects of K for Case 1 with b=2, c=5 in which we see apparent increase in d_i and d_o with decreasing the non-dimensional electro-kinetic width K. Fig. 2 shows a typical dependence of the transition distances on K, yet the detailed dependence, especially in the range of small K, is more sophisticated and is the subject of the presentation below.

RSC Advances Accepted Manuscript

This journal is © The Royal Society of Chemistry 2012

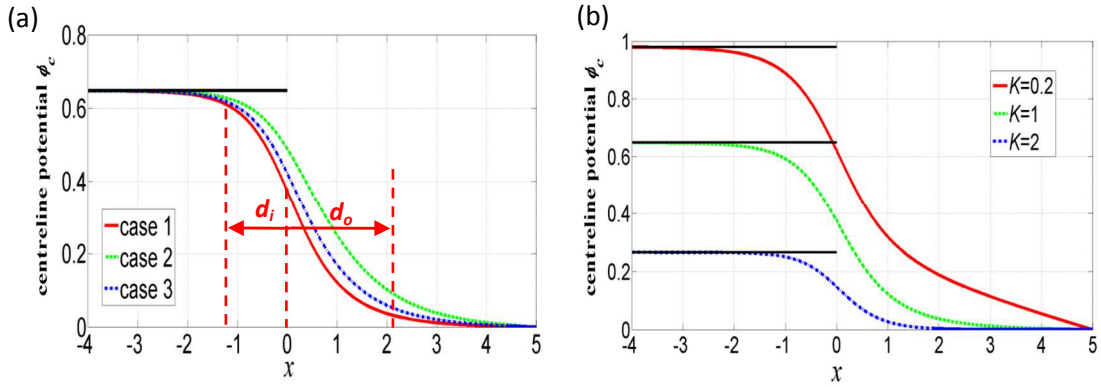

Fig 2. The centreline potential along the *x*-direction: (a) The curves from top denote, respectively, Case 2, Case 3, Case 1 with *b*=2, *c*=5, *K*=1. The top horizontal line is the asymptote $\phi_0 = 0.648$ (=1/cosh(1)) for the infinite channel; (b) The curves from top denote, respectively, *K*=0.2, 1, 2 for Case 1 with *b*=2, *c*=5 with corresponding ϕ_0=0.9803 (*K*=0.2), 0.648 (*K*=1), 0.2658 (*K*=2).

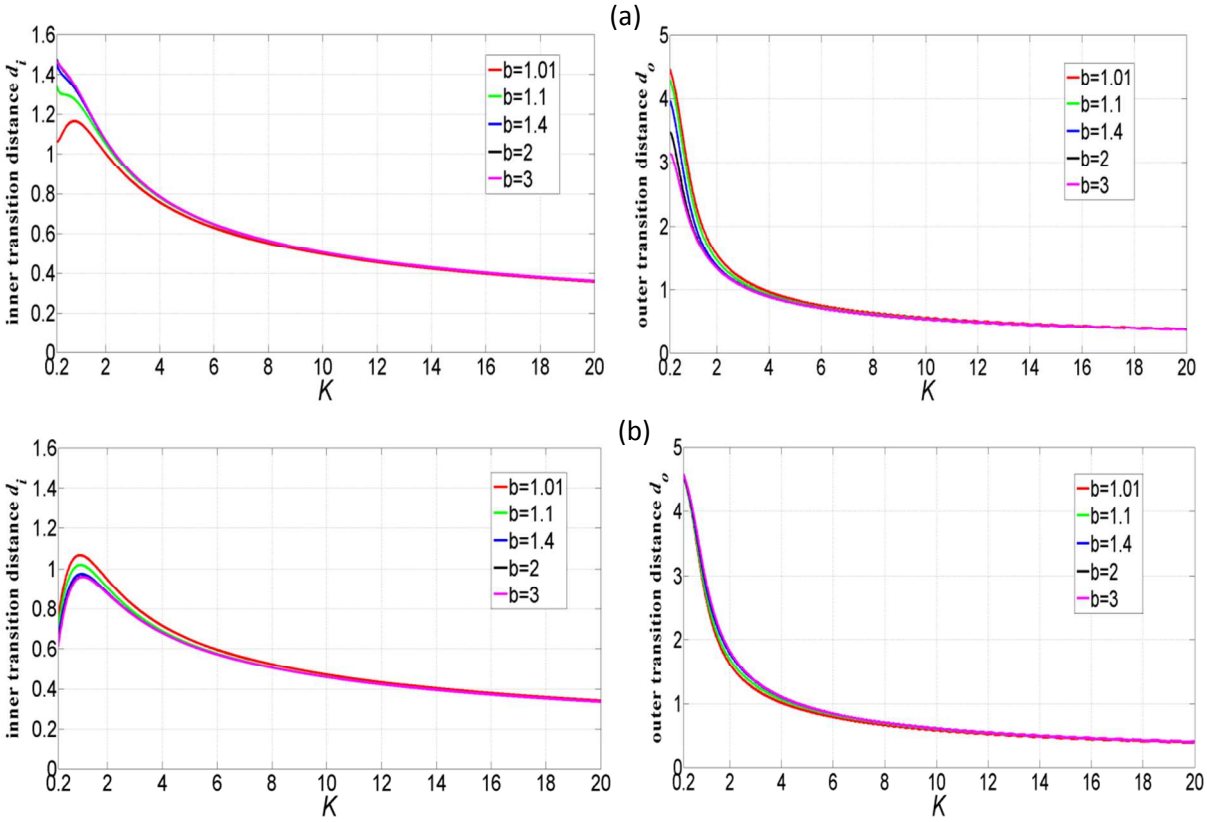

RSC Advances Accepted Manuscript

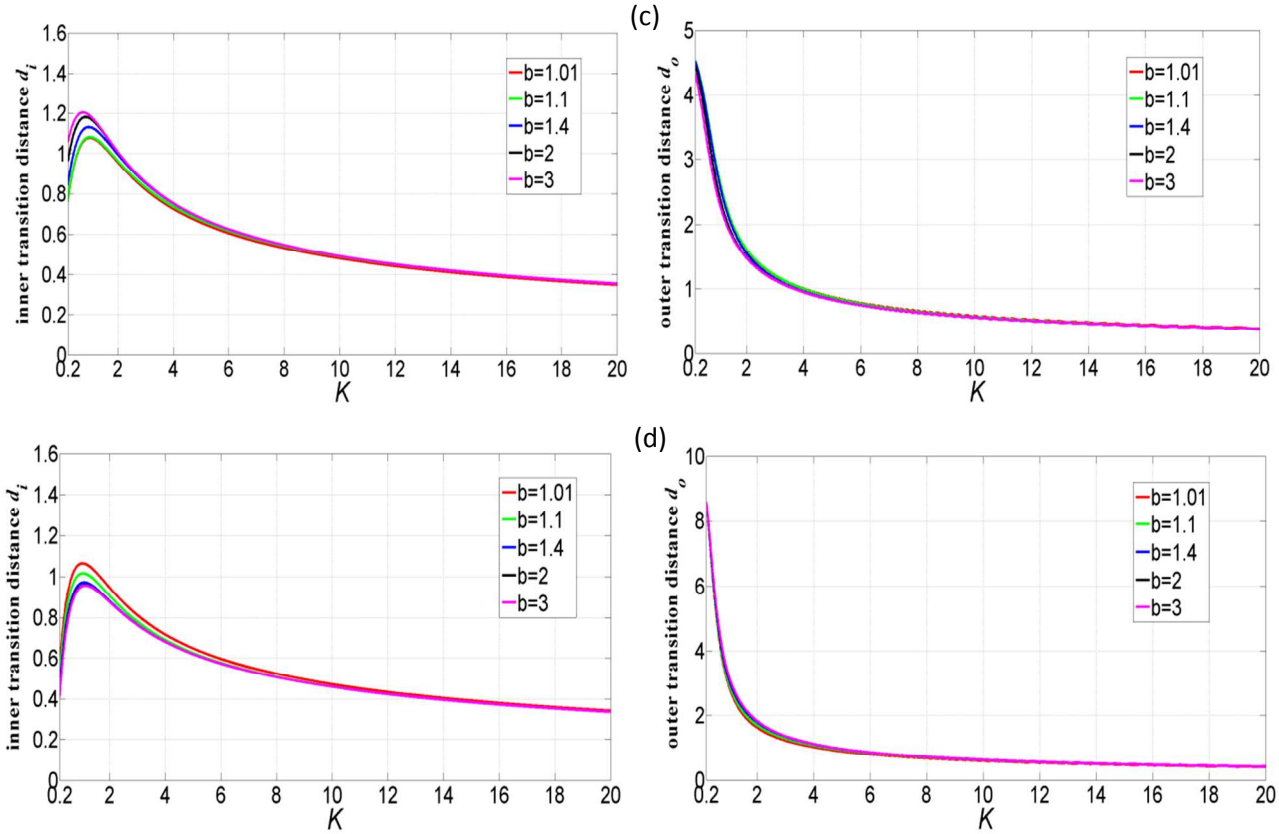

Fig 3.The transition distances versus K for various lateral periods b: (a) Case 1 (c=5); (b) Case 2 (c=5); (c) Case 3 (c=5); (d) Case 2 (c=10). The left panels show the inner transition distance d_i, while the right panels show the outer transition distance d_o. As an illustration, comparison between Case 2 (c=10) and Case 2 (c=5) shows that the reservoir distance c has small effects on the inner distance d_i, yet it has very significant influence on the outer distance d_o.

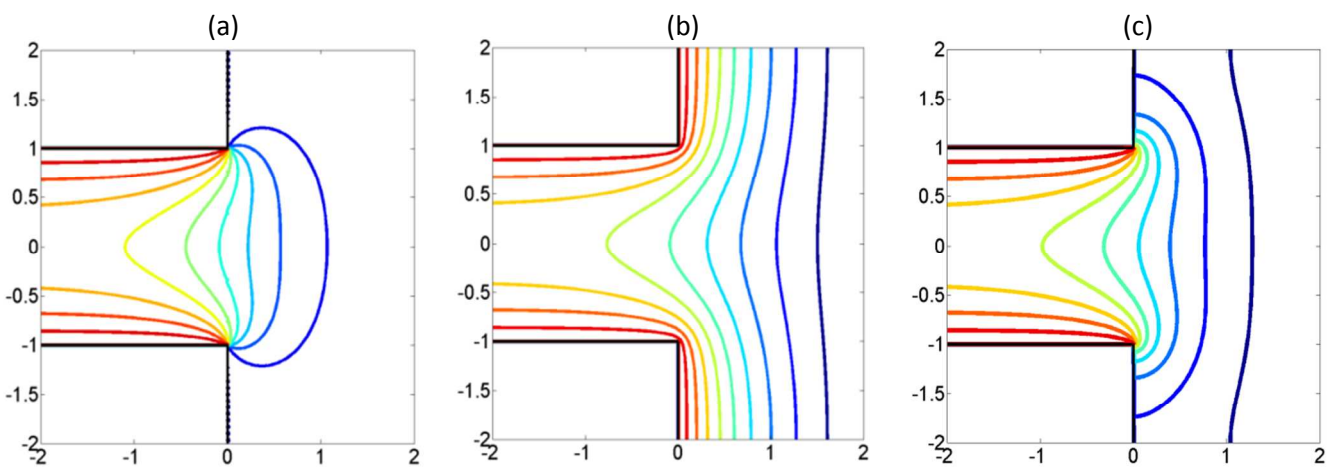

Fig 4. Typical EDL potential lines for K=1: (a) Case 1;(b) Case 2; (c) Case 3, illustrated for b=2, c=2. The difference between curves is $\Delta\phi = 0.1$. In all the three cases, the inner EDL potential patterns are quite similar while the outer EDL potential patterns look much different. Case 1, with the end-wall ϕ=0, shows a pattern of bulge from the open edge toward the reservoir. Case 2, with the end-wall ϕ=1, shows more uniform convergence from the open edge toward the reservoir. Case 2, with insulated end walls, shows an intermediate EDL pattern between Case 1 and Case 2.

RSC Advances Accepted Manuscript

This journal is © The Royal Society of Chemistry 2012

Fig. 3a-d collects results of all the three cases for c=5 with various b, and results for Case 2 with c=10 for comparison. The general features include: (1) the inner transition distance d_i is varied drastically in a range of small K, but of the order unity, has a peak at about K=1, especially in Cases 2 and 3; then decreases with increase in K, and becomes about 0.35~0.4 at the large K=20, and (2) the outer transition distance d_o is inversely proportional to K, being about the order of c for small K, then decreases with increase in K and becomes about 0.45~0.5 at the large K=20. Moreover, the results show that d_o has little dependence on the lateral period b, increasing only slightly with increase in b. The period b has more significant effects on d_i, in particular in a range of small K (say, 0.2~2) where the difference in d_i could be as large as 100% when b is varied between 1.01 and 3. In additional, we observe that the period b has opposite effects on the inner transition distances between Case 2 and Case1 & Case 3, in particular for small K; the former has a smaller d_i while the latter have a larger d_i with increasing b.

It is also of interest to see the typical EDL potential patterns and their relations to the transition distances. Fig. 4a-c shows some typical EDL potential lines for K=1, illustrated for b=2, c=2. In all the three cases, the patterns of the electrostatic potential lines inside the channel are quite similar while their patterns outside the channel look different. Case 1, with the end-wall boundary condition $\phi = 0$, shows a pattern of bulging both inward and outward from the open edge of the channel. Case 2, with the end-wall boundary condition $\phi = 1$, shows a pattern of bulging from the reservoir toward the inside of the channel. Case 3, with the insulated wall condition, shows an intermediate pattern between Case 1 and Case 2. In general, the higher degree the bulge is, the longer distance the EDL potential takes from its value of the infinite channel to the zero reservoir condition. Apparently (from the plots), these bulge behaviours are dependent upon K, and are sophisticated in the range of small $K \sim 1$, and the end-wall length (b-1) or simply the lateral period b has also important influence on the bulge depth.

Let us give some physical insight into the interesting bulge behaviours. Generally speaking, the same boundary condition may "collaborate with each other." The end-wall condition ϕ_0=0 (Case 1) will collaborate with the 0 reservoir potential to help penetration of the bulge toward the inside of the channel, while the end wall condition ϕ_0=1 (Case 2) will collaborate with the same side-wall potential to exclude the bulge from the inside of the channel. (i) When the channel is wider (K larger than, say, 6), ϕ_0=1/cosh(K) is approximately zero, thus the (smooth) transition (ϕ_c) takes a shorter distance (d_i plus d_o) from ϕ_0 to the reservoir value 0 (cf. fig 2(b)). (ii) When the channel is narrow (K smaller than, say, 1) when the two side walls are so close to each other, we have to distinguish between the three cases. Case 1 with end wall ϕ=0 presents a larger bulge, and the inner transition distance d_i for b> 1.4 typically increases with decreasing K. But for shorter end walls (1<b<1.4), collaboration between the end walls and the reservoir is weaker, the inner transition distance d_i is reduced with decreasing K. On the other hand, for Case 2 with the end-wall boundary condition ϕ=1, the side walls and the end walls collaborate to effectively exclude the bulge behaviour, thus reducing the inner entrance distance with decreasing K (as the side walls are so close to each other). Case 3 with insulated end walls again shows intermediate behaviours. It is also noted that given the reservoir distance c, none of the collaboration effects have significant effects on the outer transition distance d_o for the entire range of K (> 0.2) under investigation; yet variation of b does have some effects in Case 1 for K smaller than 4 (cf. Fig. 2a).

Concluding Remarks

In practice, all EDL channels are finite in length and have open edges. As the channel width becomes small, the EDLs on the two side walls overlap, and thus the zero reference potential does not attain in the channel, but must lie somewhere outside it. In this study, we have addressed the important issue of open-edge effects for the electrostatic EDL potential by considering three different boundary conditions on the end walls: Cases 1, 2 and 3.

The effects of the open edge on the EDL potentials are characterized by two non-dimensional transition distances. One is the inner d_i, beyond which the EDL potential deviates less than 5% from that for the infinite channel. The other is the outer d_o, beyond which the EDL potential becomes 95% close or more to the reference (zero) potential of the reservoir. The analysis, under the Debye-Hückel approximation, is pursued for all channel widths, namely, for arbitrary values of K (the non-dimensional electro-kinetic width). Nevertheless, we focus our discussion for K between 0.2 and 20,which cover a range of great interest from overlapped EDLs (say, K< 2) to well-separated EDLs (say, K>4). Two other parameters also play an important role in determining the transition distances: b, the normalized period between parallel channels, and c, the normalized distance between the open edge and the reservoir.

It is found that (1) the inner transition distance d_i is varied drastically but of the order unity for small K with peaks at about K=1, especially in Cases 2 and 3, then decreases with increase in K, and becomes about 0.35~0.4 at K=20; (2) the outer transition distance d_o is inversely proportional to K; it is of the order c for small K, then decreases with increase in K and becomes about 0.45~0.5 at K=20. Moreover, the results show that d_o has little dependence on the period b, but does increase somewhat with increase in b for Case 1. The lateral period b has more significant effects on d_i, in particular for small K (say, 0.2~2) when b is varied between 1.01 and 3. These trends have been explained, with the help of bulge behaviours observed from the plots of EDL potential lines, by the collaboration effects between the end walls and the reservoir for Case 1, and by the collaboration effects between the end walls and the side walls for Case 2. Generally speaking, Case 3 with insulated end walls shows intermediate behaviours.

The present quantitative results provide useful references to the design of channels for practical applications in micro- and nano-fluidics, especially for those intended to be operated under transient and unsteady conditions. The latter conditions require quick equilibrium in the electrostatic (EDL) potential so that full

RSC Advances Accepted Manuscript

development assumed in the steady-state analysis can be applied with greater accuracy.

Acknowledgements

The work was supported in part by the National Science Council (Taiwan) under the Contract number NSC 100-2221-E-002-152-MY3. Part of this work was completed while the first and the corresponding authors (CF Kung & CC Chang) were visiting Guangxi University, China.

Notes and references

[a]College of Mechanical Engineering, Guangxi University, Nanning 500034, China.
E-mails:mechang@gxu.edu.cn;mechang@iam.ntu.edu.tw (C.C. Chang)
[b]Department of Mathematics and Department of Mechanical Engineering, Michigan State University, East Lansing, Michigan 48824, USA
[c]Institute of Applied Mechanics, National Taiwan University, Taipei 106, Taiwan.

1 H. A. Stone, A. D. Stroock and A. Ajdari , *Ann. Rev. Fluid Mech*., 2004, **36**, 381–411.

2 C. L. Rice and R. Whitehead, *J. Phys. Chem*., 1965, **69**, 4017–4024.

3 P. X. Feng, *Surface Sci*. 1999, **429**, L469–L474.

4 C. Yang, D. Q. Li and J. H. Masliyah, *Int. J. Heat Mass Trans*.,1998, **41**, 4229–4249.

5 G. M. Mala, C. Yang and D. Q. Li, *Colloid Interface Sci. A*, 1998, **135**, 109–116.

6 C. Yang and D. Q. Li, *Colloids Surfaces A*, 1998, **143**, 339–353.

7 H. J. Keh, and Y. Y. Wu, *J. Phys. Chem. B*, 2011, **115**, 9168 – 9178.

8 Y. L. Zhang, T. K. Wong, C. Yang and K. T. Ooi, *Int. J. Eng. Sci*. 2005, **43**, 1450–1463.

9 C. F. Kung, C. Y. Wang and C. C. Chang, *Electrophoresis*, 2013, **34**, 3133–3140.

10 C. Y. Lee, G. B. Lee, L. M. Fu, K. H. Lee and R. J. Yang, *J. Micromech. Microeng.* 2004, **14**, 1390–1398.

11 K. A. Mahabadi, I. Rodriguez, S. C. Haur, J. A. van Kan, A. A. Bettioland F. Watt, *J. Micromech. Microeng.* 2006, **16**, 1170–1180.

12 C. T. Kuo and C. H. Liu, *Lab Chip*, 2008, **8**, 725–733.

13 A. Plecis, J. Tazid, A. Pallandre, P. Martinhon, C. Deslouis, Y. Chen and A. M. Haghiri-Gosnet, *Lab Chip*, 2010, **10**, 1245–1253.

14 D. Fine, A. Grattoni, E. Zabre, F. Hussein, M. Ferrari and X. Liu, *Lab Chip*, 2011, **11**, 2526–2534.

15 J. E. Hall, *J. Gen. Physiol*., 1975, **66**, 531–532.

16 D. G. Luchinsky, R. Tindjong, I. Kaufman, P. V. E. McClintock and R. S. Eisenberg, *Phys. Rev. E*, 2009, **80**, 021925.

17 C. Y. Wang and C. C. Chang, *Electrophoresis*, 2007, **28**, 3296–3301.

18 C. Y. Wang, Y. H. Liu and C. C. Chang, *Physics of Fluids*, 2008, **20**, 063105.

19 H. Bruus, Theoretical Microfluidics, fall 2005, second edition, Department of Micro and Nanotechnology Technical University of Denmark.

RSC Advances Accepted Manuscript

This journal is © The Royal Society of Chemistry 2012